ELECTRONIC SUPPLEMENTARY INFORMATION

Direct observation of an equilibrium between two anion-cation orientations in olefin Pt(II) complex ion pairs by HOESY NMR spectroscopy

Alceo Macchioni,*[a] Alessandra Magistrato,[b] Ida Orabona,[c] Francesco Ruffo,[c] Ursula Röthlisberger,[b] and Cristiano Zuccaccia[a]

[a]*Dipartimento di Chimica, Università di Perugia, Via Elce di Sotto, 8, 06123 Perugia. Italy. E-mail: alceo@unipg.it; Fax: (+39) 075 5855598.*

[b]*Laboratory of Inorganic Chemistry, ETH-Zentrum, Hönggerberg CH-8093 Zürich, Switzerland.*

[c]*Dipartimento di Chimica, Università di Napoli "Federico II", Complesso Universitario di Monte S. Angelo, Via Cintia, 80126, Napoli, Italy.*

NMR intramolecular characterization

The intramolecular characterization of complexes **1** - **3** was carried out by ^{1}H, ^{13}C, ^{19}F, ^{1}H-COSY, ^{1}H-NOESY, ^{19}F,^{1}H-HOESY, ^{1}H,^{13}C HMQC NMR. The ^{1}H-NOESY spectrum of complexes shows exchange peaks at 302K: CH(Md) with CH(Ou), CH(Mu) with CH(Od), Me(Mdf) with Me(Ouf), Me(Mdb) with Me(Oub), Me(Muf) with Me(Odf), Me(Mub) with Me(Odb) and Me(M) with Me(O) (Scheme 1S). By lowering the temperature down to 277K the exchange peaks disappear and all the resonances could be assigned.

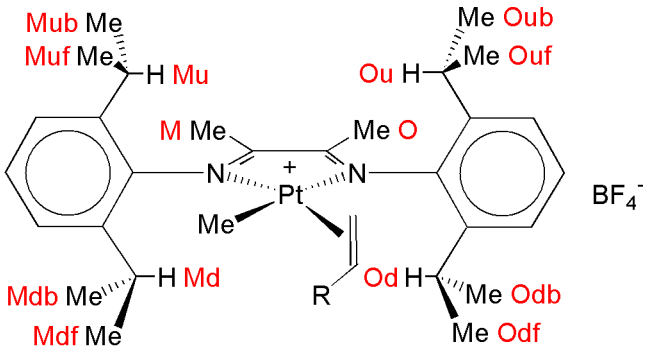

R = C_6H_5 (**1**), 4-(CH_3)C_6H_4 (**2**), 4-(CF_3)C_6H_4 (**3**)

Scheme 1S "M" and "O" indicate groups that stay in *cis* position with respect to Methyl and Olefin groups, respectively. "u" and "d" discriminate the up and down methyl orientations with respect to the olefin R group. Finally, "b" and "f" stand for backward and forward with respect to the plane containing the two phenyl groups (assumed to be co-planar).

Characterization of complex 1

^{1}H NMR(400 MHz, chloroform-d, 25°C, TMS): δ = 7.40 (m, 3H; N,N-aromatics cis with respect to olefin), 7.37 (m, 2H; *o*H olefin), 7.32 (m, 1H; *p*H olefin), 7.26 (m, 2H; *m*H olefin), 7.24 (m, 3H; aromatics cis with respect to Me), 5.76 (m, ^{3}J(H,H) = 14.3 Hz, ^{3}J(H,H) = 8.2 Hz, ^{2}J(Pt,H) = 85.7 Hz, 1H; RC*H*=CH_2), 4.07 (m, ^{3}J(H,H) = 14.3 Hz, ^{2}J(Pt,H) = 56.2 Hz, 1H; RCH=C$H_{2(trans)}$), 3.36 (m, ^{3}J(H,H) = 8.2 Hz, ^{2}J(Pt,H) = 35.9 Hz, 1H; RCH=C$H_{2(cis)}$), 3.28 (sept, ^{3}J(H,H) = 6.8 Hz, 1H; CH(Od)), 3.19 (sept, ^{3}J(H,H) = 6.8 Hz, 1H; CH(Ou)), 3.15 (sept, ^{3}J(H,H) = 6.8 Hz, 1H; CH(Md)), 2.81 (sept, ^{3}J(H,H) = 6.8 Hz, 1H; CH(Mu)), 2,52 (s, 3H; CH_3(M)), 2.36 (s, 3H; CH_3(O)), 1.492 (d, ^{3}J(H,H) = 6.8, 3H; CH_3(Odf)), 1.490 (d, ^{3}J(H,H) = 6.8, 3H; CH_3(Ouf)), 1.37 (d, ^{3}J(H,H) = 6.8, 3H; CH_3(Odb)), 1.30 (d, ^{3}J(H,H) = 6.8, 3H; CH_3(Mdb)), 1.28 (d, ^{3}J(H,H) = 6.8, 3H; CH_3(Muf)), 1.21 (d, ^{3}J(H,H) = 6.8, 3H; CH_3(Mub)), 1.18 (d, ^{3}J(H,H) = 6.8, 3H; CH_3(Oub)), 0.95 (d, ^{3}J(H,H) = 6.8, 3H; CH_3(Mdf)), -0.24 (m, ^{2}J(Pt,H) = 71.6, 3H; CH_3). ^{13}C NMR(400 MHz, chloroform-d, 25°C, TMS): δ = 186.9 (s, 1C; C=N(M)), 179.3 (s, 1C; C=N(O)), 140.9 (s, 1C; *o*C(Md)), 140.7 (s, 1C; *o*C(Od)), 139.5 (s, 1C; *o*C(Mu)), 139.4 (s, 1C; *o*C(Ou)), 139.3 (s, 1C; C-N(M)), 137.4 (s, 1C; C-N(O)), 136.1 (q, 1C; C_{ipso} olefin), 130.6 (s, 1C; *p*C olefin), 129.1 (s, 1C; *m*C olefin), 129.0 (s, 1C; *o*C olefin) 129.6, 125.7, 124.9 (s, 3C; aromatics cis with respect to olefin), 129.5, 125.0, 124,1 (s, 3C; cis with respect to Me), 96.8 (s, 1C; R*C*H=CH_2), 61.7 (s, 1C; RCH=*C*H_2), 29.3 (s, 1C; CH(Mu)), 29.1 (s, 1C; CH(Ou)), 28.7 (s, 1C; CH(Od)), 28.6 (s, 1C; CH(Md)), 25.9 (s, 1C; CH_3(Odb)), 25.3 (s, 1C; CH_3(Oub)), 24.8 (s, 1C; CH_3(Odf)), 24.6 (s, 1C; CH_3(Mdb)), 24.2 (s, 1C; CH_3(Mub)), 23.7 (s, 1C; CH_3(Ouf)), 23.5 (s, 1C; CH_3(Mdf)), 23.4 (s, 1C; CH_3(Muf)), 22.9 (s, 1C; CH_3(O)), 22.1 (s, 1C; CH_3(M)), 0.92 (m, ^{1}J(Pt,C) =

720.0 Hz, 1C; CH_3). ^{19}F NMR(400 MHz, chloroform-d, 25°C, TMS): δ = -152.32, -152.37 (m, 4F; BF_4).

Characterization of complex 2

^1H NMR(400 MHz, chloroform-d, 25°C, TMS): δ = 7.39 (m, 3H; aromatics cis with respect to olefin), 7.25 (m, 3H; aromatics cis with respect to Me), 7.25 (d, $^3J(H,H)$ = 7.9 Hz, 2H; *o*H olefin), 7.08 (d, $^3J(H,H)$ = 7.9 Hz, 2H; *m*H olefin), 5.76 (m, $^3J(H,H)$ = 14.6 Hz, $^3J(H,H)$ = 8.2 Hz, $^2J(Pt,H)$ = 77.2 Hz, 1H; RC*H*=CH_2), 4.04 (m, $^3J(H,H)$ = 14.5 Hz, $^2J(Pt,H)$ = 60.8 Hz, 1H; RCH=C$H_{2(trans)}$), 3.33 (m, $^3J(H,H)$ = 8.2 Hz, $^2J(Pt,H)$ = 55.1 Hz, 1H; RCH=C$H_{2(cis)}$), 3.26 (sept, $^3J(H,H)$ = 6.7 Hz, 1H; CH(Od)), 3.19 (sept, $^3J(H,H)$ = 6.7 Hz, 1H; CH(Ou)), 3.16 (sept, $^3J(H,H)$ = 6.8 Hz, 1H; CH(Md)), 2.81 (sept, $^3J(H,H)$ = 6.7 Hz, 1H; CH(Mu)), 2,50 (s, 3H; CH_3(M)), 2.35 (s, 3H; CH_3(O)), 2.29 (s, 3H; CH_3 olefin), 1.49 (d, $^3J(H,H)$ = 6.7, 3H; CH_3(Odf)), 1.48 (d, $^3J(H,H)$ = 6.7, 3H; CH_3(Ouf)), 1.36 (d, $^3J(H,H)$ = 6.7, 3H; CH_3(Odb)), 1.30 (d, $^3J(H,H)$ = 6.8, 3H; CH_3(Mdb)), 1.28 (d, $^3J(H,H)$ = 6.7, 3H; CH_3(Muf)), 1.20 (d, $^3J(H,H)$ = 6.8, 3H; CH_3(Mub)), 1.18 (d, $^3J(H,H)$ = 6.7, 3H; CH_3(Oub)), 0.96 (d, $^3J(H,H)$ = 6.8, 3H; CH_3(Mdf)), -0.22 (m, $^2J(Pt,H)$ = 71, 3H; CH_3). ^{13}C NMR(400 MHz, chloroform-d, 25°C, TMS): δ = 186.6 (s, 1C; C=N(M)), 179.2 (s, 1C; C=N(O)), 141.1 (s, 1C; *o*C(Md)), 140.9 (s, 1C; *o*C(Od)), 140.7 (s, 1C; C_{ipso}(olefin)), 139.5 (s, 1C; *o*C(Ou)), 139.45 (s, 1C; *o*C(Mu)), 139.38 (s, 1C; C-N(M)), 137.5 (s, 1C; C-N(O)), 133.2 (s, 1C; C_{ipso} cis with respect to Me), 129.5, 125.6, 124.9 (s, 3C; aromatics cis with respect to olefin), 129.4, 125.0, 124,1 (s, 3C; aromatics cis with respect to Me), 129.8 (s, 1C; *m*C olefin), 128.1 (s, 1C; *o*C olefin), 97.8 (m, $^1J(Pt,C)$ = 168.7 Hz, 1C; R*C*H=CH_2), 61.1 (m, $^1J(Pt,C)$ = 199.0 Hz, 1C; RCH=*C*H_2), 29.3 (s, 1C; CH(Mu)), 29.1 (s, 1C; CH(Ou)), 28.7 (s, 1C; CH(Od)), 28.5 (s, 1C; CH(Md)), 25.9 (s,

1C; CH_3(Odb)), 25.3 (s, 1C; CH_3(Oub)), 24.8 (s, 1C; CH_3(Odf)), 24.6 (s, 1C; CH_3(Mdb)), 24.2 (s, 1C; CH_3(Mub)), 23.7 (s, 1C; CH_3(Ouf)), 23.5 (s, 1C; CH_3(Mdf)), 23.4 (s, 1C; CH_3(Muf)), 22.9 (s, 1C; CH_3(O)), 22.1 (s, 1C; CH_3(M)), 21.8 (s, 3C; CH_3 olefin), 0.9 (m, ^{1}J(Pt,C) = 720.0 Hz, 1C; CH_3). ^{19}F NMR(400 MHz, chloroform-d, 25°C, TMS): δ = -152.36, -152.42 (m, 4F; BF_4).

Characterization of complex 3

^{1}H NMR(400 MHz, chloroform-d, 0°C, TMS): δ = 7.53 (m, AB system, 4H; *o*H and *m*H olefin), 7.41 (m, 3H; aromatics cis with respect to olefin), 7.26 (m, 3H; aromatics cis with respect to Me), 5.66 (m, ^{3}J(H,H) = 14.1 Hz, ^{3}J(H,H) = 8.4 Hz, ^{2}J(Pt,H) = 82.2 Hz, 1H; RC*H*=CH_2), 4.09 (m, ^{3}J(H,H) = 14.1 Hz, ^{2}J(Pt,H) = 51.0 Hz, 1H; RCH=C$H_{2(trans)}$), 3.36 (m, ^{3}J(H,H) = 8.4 Hz, ^{2}J(Pt,H) = 31.0 Hz, 1H; RCH=C$H_{2(cis)}$), 3.30 (sept, ^{3}J(H,H) = 6.8 Hz, 1H; CH(Od)), 3.21 (sept, ^{3}J(H,H) = 6.8 Hz, 1H; CH(Ou)), 3.12 (sept, ^{3}J(H,H) = 6.8 Hz, 1H; CH(Md)), 2.79 (sept, ^{3}J(H,H) = 6.8 Hz, 1H; CH(Mu)), 2,54 (s, 3H; CH_3(M)), 2.36 (s, 3H; CH_3(O)), 1.48 (d, ^{3}J(H,H) = 6.8, 3H; CH_3(Ouf)), 1.45 (d, ^{3}J(H,H) = 6.8, 3H; CH_3(Odf)), 1.36 (d, ^{3}J(H,H) = 6.8, 3H; CH_3(Odb)), 1.30 (d, ^{3}J(H,H) = 6.8, 3H; CH_3(Mdb)), 1.28 (d, ^{3}J(H,H) = 6.8, 3H; CH_3(Muf)), 1.18 (d, ^{3}J(H,H) = 6.8, 3H; CH_3(Mub)), 1.16 (d, ^{3}J(H,H) = 6.8, 3H; CH_3(Oub)), 0.92 (d, ^{3}J(H,H) = 6.8, 3H; CH_3(Mdf)), -0.28 (m, ^{2}J(Pt,H) = 68.0, 3H; CH_3). ^{13}C NMR(400 MHz, chloroform-d, 25°C, TMS): δ = 187.5 (s, 1C; C=N(M)), 179.6 (s, 1C; C=N(O)), 141.2 (s, 1C; *o*C(Md)), 140.1 (s, 1C; *o*C(Od)), 139.8 (s, 1C; C_{ipso}(olefin)), 139.5 (s, 1C; *o*C(Ou)), 139.3 (s, 1C; *o*C(Mu)), 139.0 (s, 1C; C-N(M)), 137.2 (s, 1C; C-N(O)), 132.0 (q, ^{2}J(F,C) = 32.7 Hz, 1C; C_{ipso} bonded to CF_3), 129.5, 125.9, 124.9 (s, 3C; aromatics cis with respect to olefin), 129.6, 125.2, 124,1 (s, 3C; aromatics cis with respect to Me), 129.3

(s, 1C; *o*C olefin), 126.7 (q, $^{3}J(F,C)$ = 2.5 Hz, 1C; *m*C olefin), 124.0 (q, $^{1}J(F,C)$ = 272.0 Hz, 3C; CF_3), 93.2 (m, $^{1}J(Pt,C)$ = 188.0 Hz, 1C; R*C*H=CH_2), 62.4 (m, $^{1}J(Pt,C)$ = 186.8 Hz, 1C; RCH=*C*H_2), 29.4 (s, 1C; CH(Mu)), 29.3 (s, 1C; CH(Ou)), 28.5 (s, 1C; CH(Od)), 28.4 (s, 1C; CH(Md)), 25.9 (s, 1C; CH_3(Odb)), 25.3 (s, 1C; CH_3(Oub)), 24.8 (s, 1C; CH_3(Odf)), 24.6 (s, 1C; CH_3(Mdb)), 24.3 (s, 1C; CH_3(Mub)), 23.6 (s, 1C; CH_3(Ouf)), 23.5 (s, 1C; CH_3(Mdf)), 23.3 (s, 1C; CH_3(Muf)), 22.9 (s, 1C; CH_3(O)), 22.1 (s, 1C; CH_3(M)), 1.1 (m, $^{1}J(Pt,C)$ = 712.6 Hz, 1C; CH_3). ^{19}F NMR(400 MHz, chloroform-d, 0°C, TMS): δ = -63.3 (s, 3F; CF_3), -151.97, -152.02 (m, 4F; BF_4).

^{1}H and ^{19}F Pulsed Field-Gradient Spin-Echo measurements.

All the measurements were performed on a Bruker AVANCE DRX 400 spectrometer equipped with a GREAT 1/10 gradient unit and a QNP probe with a Z-gradient coil, at 296 K without spinning, for a sample prepared by dissolving complex **3** in chloroform-d (ca 4.10^{-2}M). The shape of the gradients was rectangular, their duration (δ) was 5 ms, their strength *(*G) was varied during the experiments, while the diffusion time (Δ) was 75 ms. The ^{1}H and ^{19}F NMR spectra were acquired using 32K points, 32 scans, a spectral width of 4800 Hz (^{1}H) and 46000 Hz (^{19}F), a total recycle time of 15 s and processed with a line broadening of 1 Hz. The semilogarithmic plots of $\ln(I/I_0)$ *vs* G^2 were fitted using a standard linear regression algorithm obtaining an *R* factor always better than 0.99.

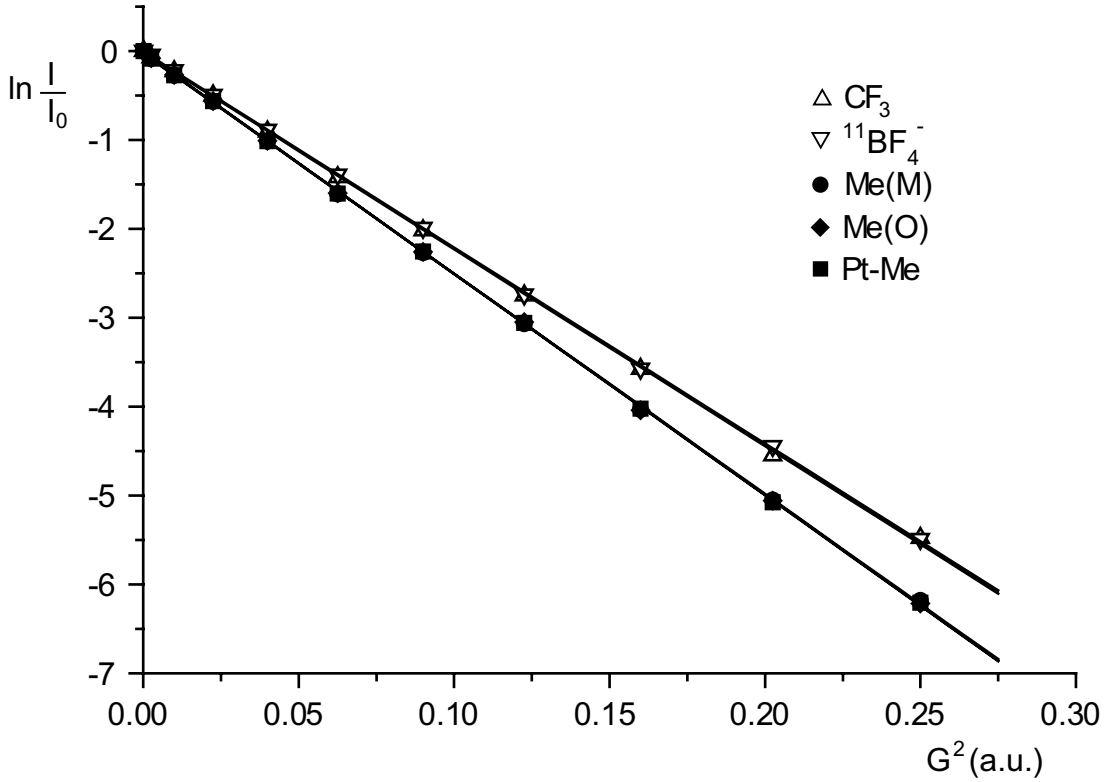

Fig. 1S Plot of $\ln(I/I_0)$ versus G^2 (a. u. arbitrary units) (where I = resonance intensity, I_0 = resonance intensity without gradient and G = gradient strength) for two ^{19}F (△ and ▽) and three ^{1}H resonances (◆, ● and ■) for compound **3**. The slope of the straightline relative to the anion is the same as that of CF_3 and those of Me(O), Me(M) and Pt-Me divided by $(\gamma_H/\gamma_F)^2$ (where γ_H and γ_F are the hydrogen and fluorine giromagnetic ratios, respectively).

Dependence of NOE on mixing time (τ_m) and temperature (T).

The $^{19}F,^{1}H$-HOESY NMR spectra for complex **3** were recorded with mixing time ranging from 0.01 to 1.6 s (Fig. 2S), digital resolution of 37.5 Hz/point in the indirect dimension, 32 scans for every increment and initial delay of 7 s with a consequent experimental time of ca 8 h.

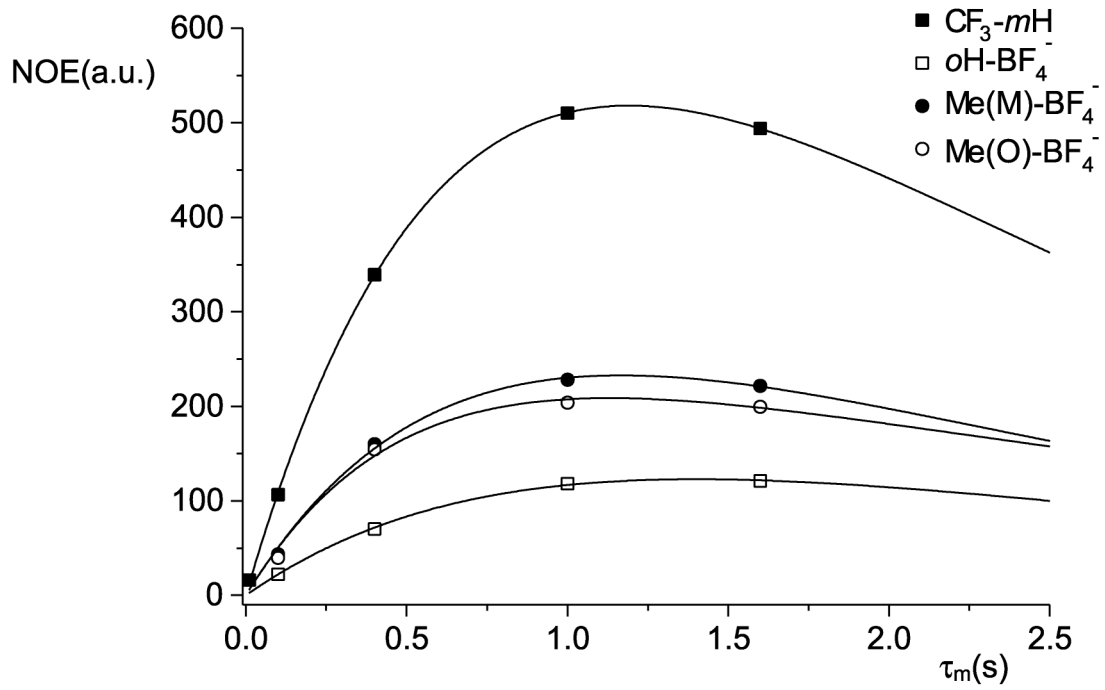

Fig. 2S Experimental trends of intramolecular and interionic NOEs, derived from the volumes of the cross peaks in the $^{19}F,^{1}H$-HOESY NMR spectra, as a function of mixing time τ_m for complex **3** (376.65 MHz, 302 K, chloroform-d).

The dependence of heteronuclear NOE on the temperature (Fig. 3S) was investigated by recording several $^{1}H,^{19}F$-HOESY NMR spectra with a mixing time of 0.2 s (Fig. 4S),

digital resolution in the direct and indirect dimensions of 2.3 and 1411.7 Hz/point, respectively, 32 scans and 7 s initial delay 1h experimental time.

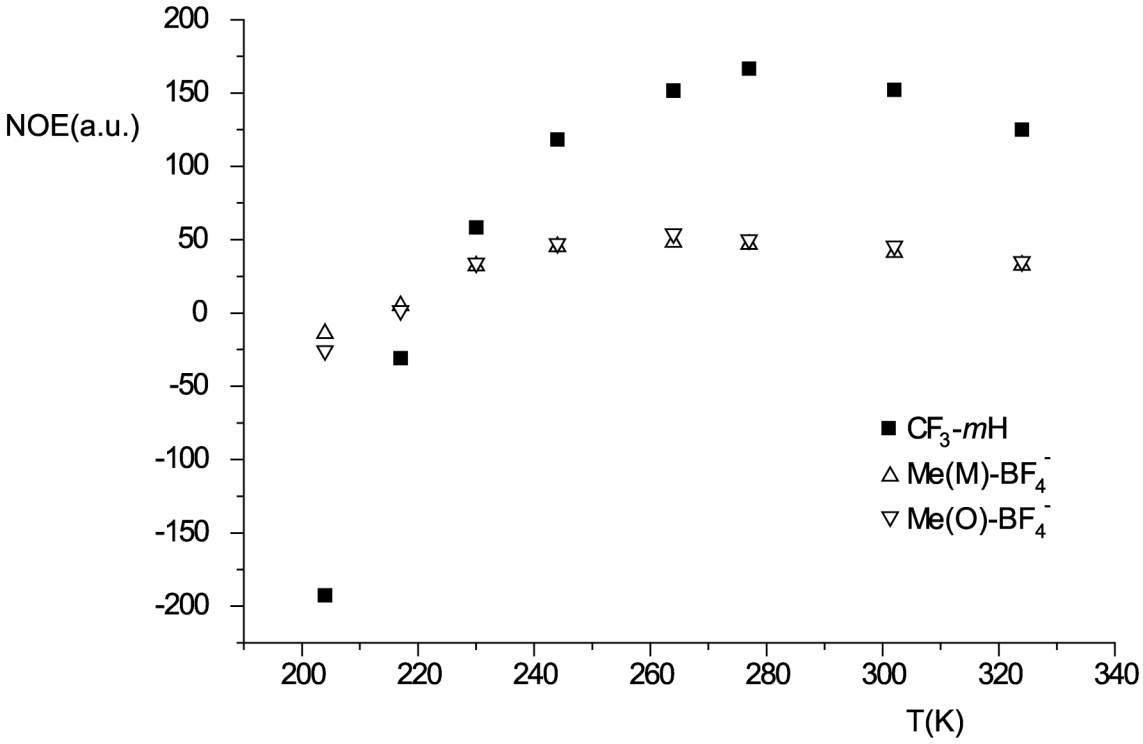

Fig. 3S Intramolecular (■) and interionic (△ and ▽) experimental NOEs as a function of temperature for complex **3**. It can be seen that the temperature values of the zero cross and maximum points are the same for both intermolecular and interionic couples of nuclei indicating the same correlation times (376.65 MHz,[D]chloroform).

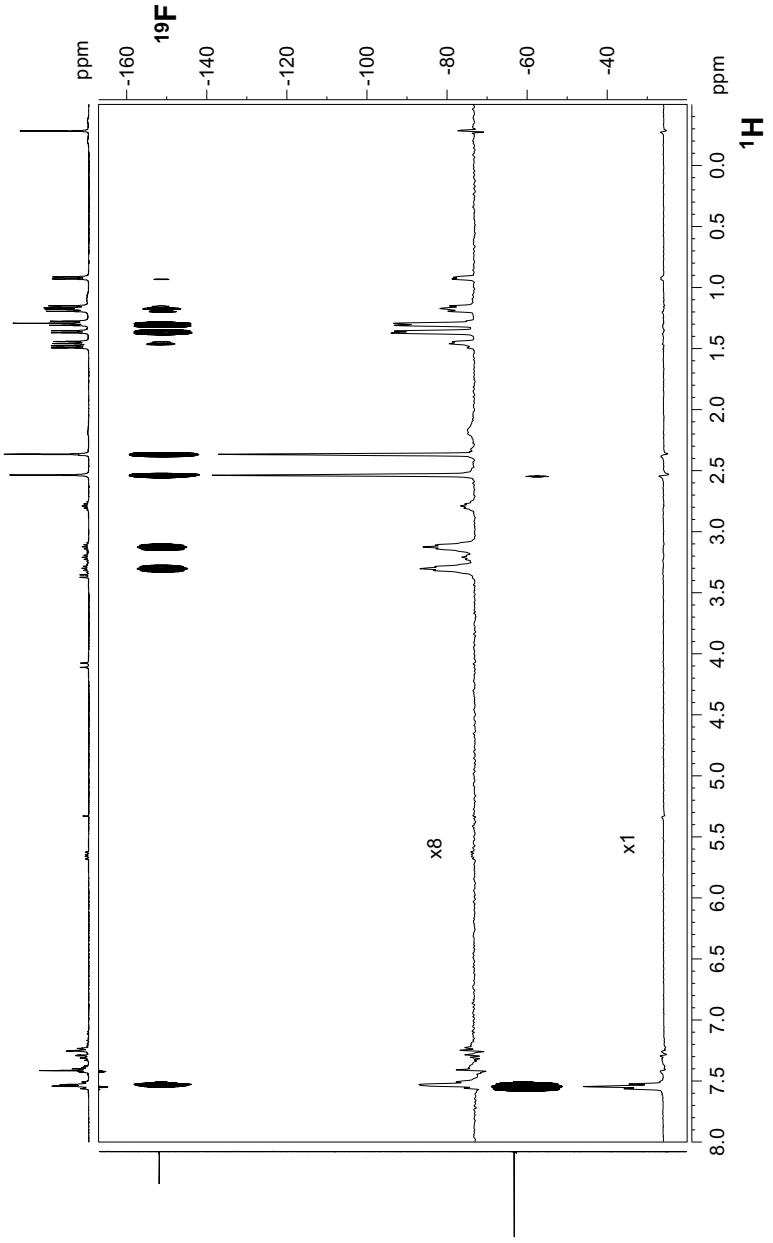

Fig. 4S $^{1}H,^{19}F$-HOESY NMR spectra recorded for complex **3** at 277 K (400.13 MHz, chloroform-d). The two 1D-traces reported on the bottom are relative to the CF_3 (x1) and BF_4^- (x8) rows.

DFT and Hybrid QM/MM Calculations

In order to determine possible reasons for the different populations of the *pseudo-cis* and *pseudo-trans* ion pairs, we performed density functional (DFT) and mixed quantum mechanics/molecular mechanics (QM/MM) calculations (with DFT as underlying electronic structure method) for compounds **3**, **1**, and **4**.[1]

Two different computational models (Fig. 5S) were used in our calculations. In both models, the two aryls substituents of the N,N-ligand were included in the MM region, while R (the substituent of the olefin) was either included in the QM or in the MM part for Model A and B, respectively.

In Model A, the inclusion of R in the QM part allows of its electronic effects on the thermodynamic stability of the ion pair to be taken into account explicitly. In contrast, in Model B, the description of R is limited to bonded and van der Waals interactions as described within the MM framework.

All our calculations were performed in gas phase starting from the X-ray structure of the unsubstituted (R = H) analogue of the complexes under investigation. First, the cationic organometallic fragment and the anion were optimized separately with full DFT calculations. Then, an initial geometry of the ion pair was constructed by positioning the anion close to van der Waals contact of the cationic complex so as to maximize electrostatic interactions between the counter ion and the organometallic fragment.

Several minima were located for both the *pseudo-cis* and *trans* configurations of the three complexes. For all of these, we optimized the structure of the ion pairs starting with different initial configurations in which the distance between the central metal and the boron atom of the counter ion was decreased slowly in increments of 0.1 Å to allow for structural relaxation. In Table 1S, we report the results relative to the most stable minimum localized for each ion pair in both QM/MM models.[2]

As shown in Table 1S, in Model A, the positioning of the counterion in *pseudo-cis* position is most the thermodynamically stable form for all complexes in agreement with the experimentally observed stability order. The relative thermodynamic stability of the *pseudo-cis* with respect to the *trans* ion pair varies as -8.7, -6.7 and -2.5 kj/mol for complexes **3**, **1** and **4**, respectively.[3] In Model B on the other hand, the *pseudo-cis* ion pair is disfavoured with respect to the *pseudo-trans* form by 1.7 and 2.9 and 4.6 kj/mol for complexes **3**, **1** and **4**. Model A and B only differ in the explicit inclusion/exclusion of the electronic effects of R. It appears that the relative thermodynamic stabilities of *pseudo-cis* and *trans* ion pairs are crucially affected by the electronic influence of this substituent.

In order to further analyze the influence of the electronic features of R on the stability of the two ion pairs, we performed an analysis of the charge distribution[4] on a full QM model of the cationic complexes. As shown in Table 2S (labeling scheme given in Scheme 1S), the charge distribution of the three organometallic fragments is almost identical. For all complexes, the methyl groups Me(M) and Me(O) and carbon atoms C(M) and C(O) present a partial positive charge, while Me bears an almost vanishing, slightly negative charge. The presence of a partial positive charge on the two methyl groups of the N,N diimine ligand could give a possible explanation for the fact that the anion was observed to be preferentially in *trans* position with respect to the olefin ligand.

Tiny differences in the charge distributions of the three complexes can be observed for R.[5] In fact, positive charges of 0.39 e, 0.20 e and 0.05 e for **3**, **1** and **4**, respectively were found. However, the total charge of the olefin does not completely account for the charge distribution induced by different olefinic ligands R. Therefore, in Table 2S, we

also report the charge that is accumulated on different parts of the olefin: i.e. on the double bond (without R), R^6 and on its *para* substituent (in **3**). In complex **3**, the double bond features a positive charge of 0.27 e, while it is essentially neutral in **1** and **4**. Furthermore, the phenyl group of complexes **3** and **1** is positively charged (0.13 e), while R=CH_3 in **4** shows a vanishing, slightly negative charge. Finally, CF_3 in **3** bears a negative charge of -0.1 e. Therefore, a small positive charge of 0.39 e (neglecting CF_3 in **3**) is accumulated on CH_2=CHR, versus 0.20 e and 0.05 e of **1** and **4**, respectively.

We also calculated the dipole moments of the free olefins (Table 3S). As shown in Table 3S, the *para*-trifluoromethyl-styrene presents the largest value of the dipole moment (4.0 D), and this value decreases successively for styrene (0.8 D) and for propylene (0.4 D). Therefore, Tables 2S and 3S clearly show that the relative thermodynamic stability of the *pseudo-cis* ion pair (with respect to the *pseudo-trans*) is strongly correlated with the charge distribution and the dipole moments of the olefins.

Thus, our results suggest that the differences in the relative thermodynamic stabilities of the *pseudo-cis* versus the *pseudo-trans* ion pairs of complexes could originate from an interaction between the anion with the positive charge accumulated on the olefin ligand. In fact, in Model A, in *pseudo-cis* position the anion is much closer to the olefin (the distance[6] between BF_4^- and the *ortho*-proton of the phenyl ring is 4.4 Å and 4.2 Å for **3** and **1**, respectively, while the distance between BF4 and the methyl of the propylene is of 6.0 Å) than in *pseudo-trans* position (8.6Å and 8.5 Å for **3** and **1**, respectively and 8.8 Å for **4**). This should maximize the electrostatic interaction between the anion and the partial positive charge of R for **3** and **1**. However due to the calculated differences in the dipole moments (i.e. in the charges of the olefin) this interaction is stronger in complex **3**. In contrast, when only non-bonded and van der Waals interactions between

R and the rest of the complex are considered, the *pseudo-cis* ion pair is disfavoured simply due to a larger steric hindrance below the coordination plane. Therefore, neglecting electrostatic interactions between R and BF_4^-, the *pseudo-trans* ion pair is favoured and the variations of ΔE for the three complexes can be attributed only to the differences in steric hindrance of R.

Computational Details

All the DFT calculations were performed using the Amsterdam Density Functional (ADF2000.01) program.[7] The electronic configurations of the molecular systems were described by a triple-STO basis set on the transition metal center for the ns, np, nd, (n+1)s and (n+1)p valence shells, whereas a double-STO basis set was used for F (2s, 2p), C (2s 2p), N (2s, 2p), B (2s, 2p) and H(1s). The inner shells of the atoms were treated within the frozen core approximation. Gradient corrected calculations with the exchange functional of Becke[8] and the correlation functional of Perdew[9] were used. First-order scalar relativistic corrections[10] were included for the platinum atom. A spin-restricted formalism was used throughout all the calculations.

The Tripos 5.2 force field[11] was used for the molecular mechanics potential, augmented for Pt and B according to the Universal force field of Rappé et al.[12] The dispersion coefficients of the Tripos[11] force field for the atoms involved were parameterised according to the Amber force field.[13] This procedure was adopted since the default van der Waals parameters of the Tripos force field were strongly overestimating the repulsive interactions, inducing large structural distortions.

Table 1S Relative thermodynamic stabilities (kJ/mol) of complexes **3**, **1**, and **4** calculated with Model A and B, respectively

	Complex **3**		Complex **1**		Complex **4**	
	cis	*trans*	*cis*	*trans*	*cis*	*Trans*
Model A	0.0	8.7	0.0	6.7	0.0	2.5
Model B	0.0	-1.7	0.0	-2.9	0.0	-4.6

Table 2S Charge distribution (in elementary charge units) for **3**, **1**, and **4**. The corresponding atom labelling scheme is reported in Scheme 1S

Group	Complex **3**	Complex **1**	Complex **4**
Pt	0.63	0.65	0.62
N(M)	-0.62	-0.63	-0.61
N(O)	-0.57	-0.57	-0.57
CH_2=CH-R	0.39	0.20	0.05
CH_2=CH-	0.27	0.07	0.07
R	0.12	0.13	-0.02
CF_3	-0.10		
Me	-0.03	-0.09	-0.09
C(M)	0.25	0.24	0.24
Me(M)	0.18	0.22	0.21
C(O)	0.24	0.24	0.24
Me(O)	0.17	0.19	0.19

Table 3S Dipole moments (in Debye) of the olefin ligands in **3**, **1**, and **4**

R	Dipole Moments
p-CF_3-Ph	4.0
Ph	0.8
Me	0.4

References

1 The olefin ligand is *para*-CF_3-styrene, styrene, and propylene, in **3**, **1**, and **4**, respectively.

2 The energy differences involved between different minima (0.5 kcal/mol for a difference of 0.5 Å in the B-Pt distance) are most certainly beyond the limit of accuracy of density functional calculations. However, we expect fortuitous error cancellation to be particularly effective in comparing these structures. In addition, the structural parameters derived from this minimization are in agreement with the experimental NOE's data.

3 Our calculations slightly overestimated the energy differences observed experimentally (ca. 2-4 kJ/mol) between pseudo-*cis* and *trans* ion pairs. In addition, entropy effects that might be important in these kinds of systems, are totally neglected. Therefore experimental free energies might not be directly comparable to the calculated enthalpies. Furthermore, our calculations are probably accurate enough to reproduce the relative thermodynamic stabilities of the pseudo-*cis* and *trans* ion pairs (experimentally of the order of 2-3 kJ/mol). However, more subtle variations within complexes **1**, **2** and **4** (experimental differences of the order of 1 kJ/mol only) are most probably beyond the accuracy limit of our calculations. In fact, we expect that error cancellation might be more effective when comparing the relative energies of the pseudo-*cis* and *trans* ion pairs, whereas we expect this to be less effective when comparing the relative energies among complexes **1**, **2** and **4**. In the latter case in fact we are comparing different chemical systems with different numbers of electrons.

4 The calculation of the Mulliken charge distribution was performed with a double-ζ basis without polarization functions for all atoms.

5 Due to the limited accuracy of calculated point charges, they cannot be expected to yield accurate absolute values, but they should supply reasonable indications about the relative trends.

1 The distances reported here refer to an average distance between the four fluorine atoms of BF_4^- and the *ortho*-proton of the olefin in **3** and **1**. For complex **4** we report the average distances between the protons of the methyl of the propylene and the four fluorine atoms of BF_4^-.

2 E. J. Baerends, D. E. Ellis and P. Ros, *Chem. Phys.*, 1973, **2**, 41. L. Versluis and T. Ziegler, *J. Chem. Phys.*, 1998, **88**, 322. G. te Velde and E. J. Baerends, *J. Comp. Phys.*, 1992, **99**, 84. C. Fonseca Guerra, J. G. Snijders, G. te Velde and E. J. Baerends, *Theor. Chim. Acc.*, 1998, **99**, 391.

3 A. Becke, *Phys. Rev. A.*, 1988, **38**, 3098.

4 J. P. Perdew and A. Zunger, *Phys. Chem. Rev. B*, 1981, **23**, 5048.

5 J. G. Snijeders and E. J. Baerends, *J. Mol. Phys.*, 1978, **36**, 1789. J. G. Snijeders, E. J. Baerends and P. Ros, *Mol. Phys.*, 1979, **38**, 1909.

6 M. Clark, R. D. Cramer III and N. van Opdenbosh, *J. Comp. Chem.*, 1989, **10**, 982.

7 A. K. Rappé, C. J. Casewit, K, S. Colwell, W. A. Goddard III and W. M. Skiff, *J. Am. Chem. Soc.*, 1992, **114**, 10024.

8 The empirical dispersion coefficients that were used for H, C, F and N are taken from the Amber force field (V. D. Cornell, P. Cieplak, C. I. Bayly, I. R. Gould, K. M. Merz Jr., D. M. Ferguson and D. C. Spellmeyer, *J. Am. Chem. Soc.*, 1995, **118**, 5179).

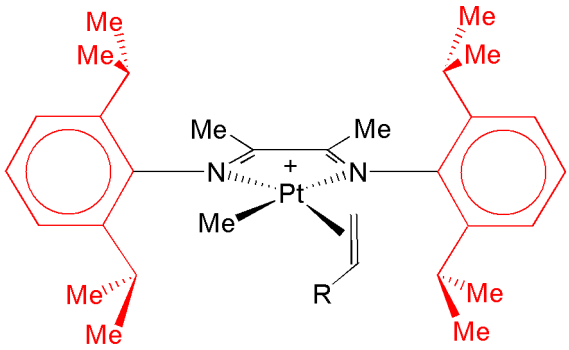

MODEL A

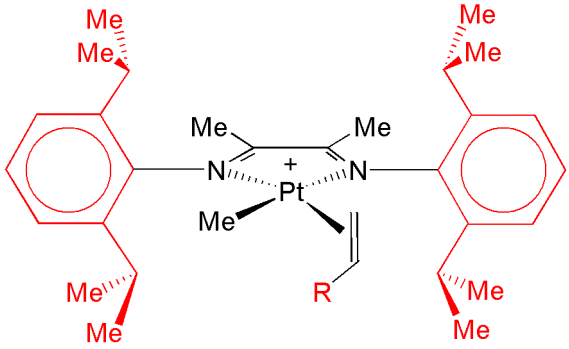

MODEL B

Fig. 5S QM/MM Model A and B. The black and the red lines correspond to the part of the complex that is included in the QM and MM part, respectively.